Pergamon

Geochimica et Cosmochimica Acta, Vol. 65, No. 14, pp. 2257–2271, 2001

0016-7037/01 $20.00 + .00

PII S0016-7037(01)00596-8

Temperature-dependent oxygen and carbon isotope fractionations of biogenic siderite

CHUANLUN L. ZHANG,[1] JUSKE HORITA,[2] DAVID R. COLE,[2] JIZHONG ZHOU,[3] DEREK R. LOVLEY,[4] and TOMMY J. PHELPS[3]

[1]Department of Geological Sciences, University of Missouri, Columbia, MO 65211, USA [2]Chemical and Analytical Sciences Division, [3]Environmental Sciences Division, Oak Ridge National Laboratory, Oak Ridge, TN 37831, USA [4]Department of Microbiology, University of Massachusetts, Amherst, MA 01003, USA

(*Received August* 7, 2000; *accepted in revised form February* 20, 2001)

Abstract—Isotopic compositions of biogenic iron minerals may be used to infer environmental conditions under which bacterial iron reduction occurs. The major goal of this study is to examine temperature-dependent isotope fractionations associated with biogenic siderite ($FeCO_3$). Experiments were performed by using both mesophilic (<35°C) and thermophilic (>45°C) iron-reducing bacteria. In addition, control experiments were performed to examine fractionations under nonbiologic conditions.

Temperature-dependent oxygen isotope fractionation occurred between biogenic siderite and water from which the mineral was precipitated. Samples in thermophilic cultures (45–75°C) gave the best linear correlation, which can be described as $10^3 \ln\alpha_{\text{sid-wt}} = 2.56 \times 10^6\ T^{-2}\ (K) + 1.69$. This empirical equation agrees with that derived from inorganically precipitated siderite by Carothers et al. (1988) and may be used to approximate equilibrium fractionation. Carbon isotope fractionation between biogenic siderite and CO_2, based on limited data, also varied with temperature and was consistent with the inorganically precipitated siderite of Carothers et al. (1988). These results indicate that temperature is a controlling factor for isotopic variations in biogenic minerals examined in this study.

The temperature-dependent fractionations under laboratory conditions, however, could be complicated by other factors including incubation time and concentration of bicarbonate. Early precipitated siderite at 120-mM initial bicarbonate tended to be enriched in ^{18}O. Siderite formed at <30 mM of bicarbonate tended to be depleted in ^{18}O. Other variables, such as isotopic compositions of water, types of bacterial species, or bacterial growth rates, had little effect on the fractionation. In addition, siderite formed in abiotic controls had similar oxygen isotopic compositions as those of biogenic siderite at the same temperature, suggesting that microbial fractionations cannot be distinguished from abiotic fractionations under conditions examined here. *Copyright © 2001 Elsevier Science Ltd*

1. INTRODUCTION

The oxygen isotope composition of sedimentary rocks may provide clues to paleoclimate changes and the evolution of oceans. The interpretation of natural variations in $^{18}O/^{16}O$, however, depends on the knowledge of how temperature and other factors affect the isotopic fractionation between a mineral and water or between coprecipitating minerals. So far, constraints on the magnitude of oxygen isotope fractionation between siderite and water include three theoretical calculations and two experimental studies (Fig. 1). Becker and Clayton (1976) calculated the equilibrium fractionation between siderite and water by using a combination of spectroscopic and thermodynamic data constrained by experimental observations. Golyshev et al. (1981) calculated fractionations by using a physical lattice model, which were similar to those of Becker and Clayton (1976). Zheng (1999) calculated fractionations by using an increment model, which were systematically greater than those of Becker and Clayton (1976) (Fig. 1). Carothers et al. (1988) first measured the fractionation between inorganically precipitated siderite and water at 33 to 197°C, which varied between the calculated values of Becker and Clayton (1976) and Zheng (1999) (Fig. 1). Mortimer and Coleman (1997) examined the fractionation between biogenic siderite and water at 18 to 40°C in a bacterial culture, which was significantly smaller than fractionations obtained from theoretical calculations or inorganic precipitation (Fig. 1).

The formation of siderite in many natural environments has been interpreted to be microbially mediated (Coleman and Raiswell, 1993; Curtis et al., 1986; Duan et al., 1996; Ellwood et al., 1988; Moore et al., 1992; Mozley and Carothers, 1992; Pye et al., 1990). However, interpretation of the oxygen isotope signatures of diagenetic siderite in the low-temperature sedimentary environments is complicated (e.g., Mozley and Carothers, 1992; Mozley and Wersin, 1992; Mortimer and Coleman, 1997). In particular, the exceptionally low $\delta^{18}O$ values (e.g., <25‰ vs. SMOW) of siderite have been explained as the result of microbially mediated processes (Mortimer and Coleman, 1997). This is intriguing because many previous interpretations of meteoric water diagenesis in marine sediments could have been invalid (Mortimer and Coleman, 1997).

Our goal is to understand the temperature-dependent oxygen isotope fractionation in the context of bacterial growth and solution chemistry. We chose several species of bacteria over a temperature range of 10 to 75°C because bacterially mediated iron reduction and siderite formation has been reported at these temperatures (Lovley, 1991; Zhang et al., 1997; Fredrickson et al., 1998; Zhang et al., 1999). Although low-temperature (<45°C) formation of biogenic siderite is typical of marine and freshwater environments (Lovley, 1991; Nealson and Saffarini, 1994), higher-temperature (>45°C) formation of biogenic siderite indicates microbial contribution to iron reduction in

Author to whom correspondence should be addressed (zhangcl@missouri.edu).

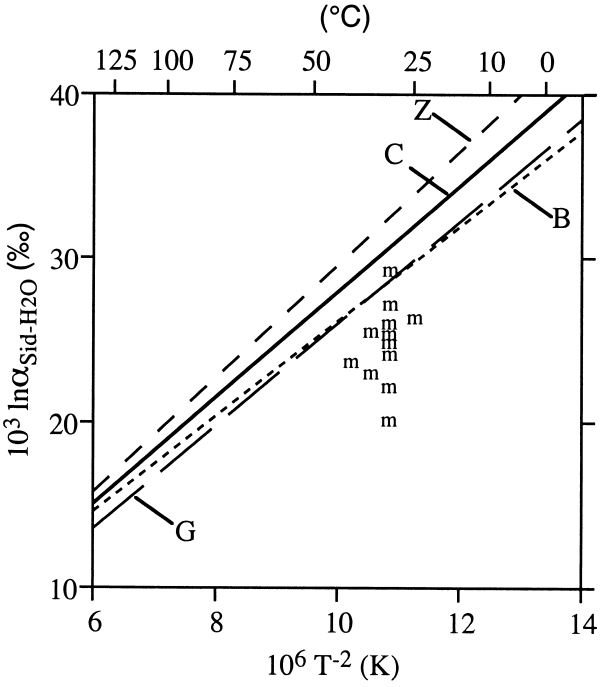

Fig. 1. Oxygen isotope fractionations as a function of temperature determined by theoretical calculations (B, Becker and Clayton; 1976; G, Golyshev et al., 1981; Z, Zheng, 1999) and by inorganic precipitation (C, Carothers et al., 1988). Also shown are biogenic siderite (letter "m") from Mortimer and Coleman (1997).

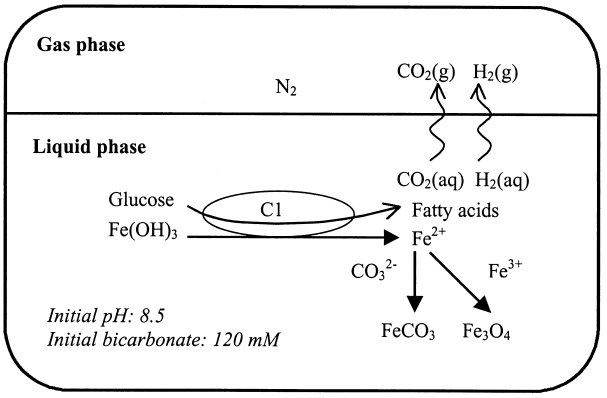

Fig. 2. A schematic diagram of the culture system in which C1 breaks down glucose into fatty acids plus H_2 and CO_2. Ferric oxyhydroxide was reduced to Fe(II), which was then precipitated as $FeCO_3$ and/or Fe_3O_4 depending on pH, redox potential, and the availability of dissolved CO_2. The source of CO_3^{2-} was mostly HCO_3^- provided at the beginning of the experiments. Fe^{3+} for magnetite precipitation was probably from the dissolution of $Fe(OH)_3$. Initial head gas was 100% N_2.

modern or ancient hot biosphere. The latter has evolutionary implications because iron reduction by thermophiles may have been the first external electron accepting process in microbial metabolism (Vargas et al., 1998).

2. MATERIALS AND METHODS

2.1. Organisms and Experimental Conditions

This study focused on a thermophilic (≥45°C) iron-reducing bacterium strain C1 because of the ease of growing this bacterium. Less emphasis was placed on two other thermophilic cultures of TOR-39 and M3-H_2, and two mesophilic cultures (10–35°C) of BrY and GS-15. Strains C1 and TOR-39 reduce iron when breaking down glucose and other carbohydrates to fatty acids plus H_2 and CO_2 (Fig. 2). Analysis using high-pressure liquid chromatography showed the presence of lactic, acetic, and propionic acids in the spent media of C1 and TOR-39 cultures (Zhang et al., unpublished data). M3-H_2 and BrY reduce iron when oxidizing H_2 or short-chain fatty acids (Caccavo et al., 1992; Liu et al., 1997; Zhang et al., 1997). Strain GS-15 reduces iron when oxidizing short-chain fatty acids or petroleum hydrocarbons (Lovley and Lonergan, 1990; Lovley and Phillips, 1988). Although these bacteria have different metabolic pathways, they all form iron minerals extracellularly. The purpose of using multiple strains in this study is to determine whether the isotopic compositions of biogenic iron minerals will be affected by bacterial species. Furthermore, growth of both mesophilic and thermophilic bacteria allows examination of temperature-dependent fractionation in a greater temperature range than using a single strain.

For this study, C1, TOR-39, M3-H_2, and BrY were cultured in a basal medium containing the following reagents (in grams per liter of deionized water): $NaHCO_3$ (2.5), NaCl (10), $MgCl_2 \cdot 6H_2O$ (0.8), $CaCl_2 \cdot 2H_2O$ (0.1), NH_4Cl (1.0), 3-[*N*-morpholino]-propanesulfonic acid (1.0), and yeast extract (0.5). Trace minerals and vitamins were added according to Phelps et al. (1989). GS-15 was cultured in a medium described by Lovley and Phillips (1988), which contained (in grams per liter of deionized water): $NaHCO_3$ (2.5), $CaCl_2 \cdot 2H_2O$ (0.1), KCl (0.1), NH_4Cl (1.5), and $NaH_2PO_4 \cdot H_2O$ (0.6). Trace minerals and vitamins were added according to Lovley et al. (1984). Both media were prepared anaerobically. The final pH was 8.2 to 8.5 for C1 and TOR-39 and ≈7.0 for M3-H_2, BrY, and GS-15. All experiments were performed in 26-mL glass tubes containing 10-mL of media that were autoclaved after preparation.

Different electron donors and gas phases were used for growing different bacterial species. C1 and TOR-39 were grown on glucose (10 mM) under a N_2 gas atmosphere; M3-H_2, and BrY were grown on hydrogen under a H_2/CO_2 (80:20 vol:vol) atmosphere; and GS-15 was grown on acetate (30 mM) under a N_2/CO_2 (80:20 vol:vol) atmosphere. The electron acceptor was ferric oxyhydroxide at ≈40 to 90 mM concentrations for C1, TOR-39, M3-H_2, and BrY. For GS-15, 250 mM of ferric oxyhydroxide is typically used in culture experiments (Lovley and Phillips, 1988) and was used here as well. Ferric citrate (≈25 mM) was used as an alternative electron acceptor for BrY.

For bacterial experiments, a 10% (vol:vol) inoculum from pregrown cultures was used. A 100-fold lower inoculum of C1 was also used when testing the effect of decreasing biomass or growth on oxygen isotope fractionation. Incubation temperatures were 45 to 75°C for C1, 65°C for TOR-39 and M3-H_2, 10 to 35°C for BrY, and 20 to 30°C for GS-15. Abiotic control experiments were performed at 65°C and 120 mM of bicarbonate, or at 95°C and 30 mM of bicarbonate by using the same medium for growing C1 and TOR-39. Table 1 summarizes the run conditions for all samples analyzed, which were categorized into 11 suites of experiments. These experiments were designed to examine different variables that may affect oxygen isotope compositions of the precipitating minerals: suites 1 to 3 mainly for time effect (0.5–720 h), suites 4 to 5 for biomass effect (0.1% or 10% inocula), suite 6 for bicarbonate effect (10–240 mM), and suites 7 to 11 for temperature (10–75°C) and bacterial species effects.

Time-course experiments were performed at 120 mM of bicarbonate to examine changes in pH, Eh, and Fe(II) as a result of bacterial growth in the C1-OR and C1-W4 cultures. Changes in pH, Eh, and Fe(II) as a result of abiotic reactions were examined in the Control-OR samples.

2.2. Bacterial Cell Counts

Bacterial cell numbers were determined by an acridine-orange direct-count method described in Zhang et al. (1996). Approximately 0.5 to 1 mL of a culture was diluted with sterile phosphate buffer (pH 7), filtered onto a black Nuclepore filter (0.2-μm pore diameter), stained with 1 mL of a particle-free acridine-orange solution for 2 min, and observed under an epifluorescence microscope.

Table 1. Experimental run conditions.

Suite	Sample type[1]	Temp (°C)	HCO_3^{-2} (mM)	Inoculum[3] (% vol:vol)	Duration[4] (h)
1	Control-OR	65, 95	120, 30	0	0.5–720, 500
2	C1-OR	65	120	10	0.5–720
3	C1-W4	65	120	10	0.5–720
4	C1-OR	65	60	0.1	3.6–240
5	C1-OR	65	60	10	3.6–240
6	C1-OR	65	10-240	10	720
7	C1-OR	45, 55, 75	120	10	720
8	C1-W4	45, 55, 75	120	10	720
9a	TOR-39-OR	65	30	10	500
9b	M3-H_2-OR	65	30	10	500
10	GS-15-UM	20, 30	30	10	500
11	BrY-OR	10, 25, 37	60	10	500

[1] OR, distilled water from Oak Ridge National Laboratory with $\delta^{18}O_{VSMOW} = -5.0‰$ to $-7.5‰$ on different dates; W4, nondistilled Antarctic water with $\delta^{18}O_{VSMOW} = -28.0‰$; UM, distilled water from University of Massachusetts with $\delta^{18}O_{VSMOW} = -9.5‰$. A C1-OR sample indicates that the culture C1 was grown in the OR water under the conditions described in the table. Control-OR indicates that bacteria were not added to the OR-water.

[2] HCO_3^- was initial concentration before an experimental run.

[3] An inoculum of 0.1% or 10% means that a 0.01-mL or 1-mL pregrown culture was added to a 10-mL medium to initiate the bacterial growth.

[4] A duration of 3.6 to 240 h means that samples were collected during incubation between 3.6 and 240 h.

2.3. Measurements of Eh, pH, and Water-Soluble Fe(II)

Measurements of Eh and pH were performed by using methods outlined in Zhang et al. (1997). The Eh was measured by placing a platinum microelectrode (Microelectrodes, Inc., Londonderry, NH) directly into the culture tube; an Eh value was recorded after equilibration for at least 5 min. The pH was then measured by transferring 5 mL of the liquid portion into a 10-mL beaker into which a pH probe was placed.

Water-soluble Fe(II) was determined by a ferrozine method modified from Zhang et al. (1997). Subsamples of 0.1 to 0.3 mL were directly added to 3-mL ferrozine (1 g/L) solution by using a needle and syringe. The sample was mixed and filtered through a Whatman syringe-filter (13-mm filter diameter, 0.2-μm pore diameter). Maximum absorbance was measured at 562 nm. Standards for the ferrozine assay were prepared with ferrous ethylenediammonium sulfate dissolved in 0.5 mol/L of HCl.

2.4. Calculations of Saturation Index and Abundance of Siderite

A MINTEQ geochemical equilibrium speciation model (Allison et al., 1991) was used to calculate ionic strength, activities of dissolved species, and the saturation index of siderite. The wt.% of siderite in the solids was calculated by using the amount of CO_2 evolved during the reaction of a subsample of a known weight (see Sec. 2.6). The percentage was then used to calculate siderite (in mg) in the total precipitate.

2.5. X-ray Diffraction and Scanning Electron Microscopy

X-ray diffraction (XRD) patterns of run products were obtained on a Scintag automated diffractometer by using cobalt Kα radiation. Samples were filtered on glass-fiber filters having a diameter of 0.45-mm, dried in an anaerobic chamber, and then measured on the diffractometer. The scan range for all samples was 2 to 70° (2θ) with a scanning rate of 2°/min. The mineralogic compositions of the sample were determined by comparing sample diffraction patterns to mineral standards provided by the International Center for Diffraction Data. The size and shape of synthesized siderite crystals were examined with a scanning electron microscope.

2.6. Analysis of Oxygen Isotopes

Natural siderite samples are typically roasted or treated with plasma or NaOCl solutions to remove labile organic matter that might cause inaccurate isotopic results (Bahrig, 1989; Moore et al., 1992; Fisher et al., 1998). Siderite in bacterial cultures, however, is among a mixture of minerals (ferric oxyhydroxide, siderite and magnetite), organic chemicals (glucose and degradation fatty acids), and biomass. The effects of roasting or chemical treatments on biogenic siderite were not known. We examined the effects of such oxidative treatments on $\delta^{18}O$ and $\delta^{13}C$ of both naturally occurring siderite and laboratory-produced biogenic siderite using glucose and spent medium (Table 2). Because magnetite has much lower $\delta^{18}O$ values than coexisting siderite (Becker and Clayton, 1976; Zhang et al., 1997), the effects of magnetite (both commercial and biogenic) on isotope compositions of siderite were also evaluated (Table 2). Finally, because glass fibers were used in the reaction vessels to prevent the loss of sample during evacuation, the effects of glass fibers on isotope compositions of siderite were evaluated as well. Possible contamination from organic carbon was checked by examination of mass spectrum after each isotopic run.

The natural siderite was a single crystal ($3 \times 3 \times 2$ cm^3) that appeared to be pure $FeCO_3$ based on analysis of X-ray diffraction (data not shown). A portion of the crystal was ground to particles of $\leq$10-μm in size before isotopic analysis. The biogenic siderite comprised fine-grained particles (3–5 μm) coprecipitated with submicron-sized magnetite in a TOR-39 culture (Zhang et al., 1998). Treatments of the natural and biogenic siderite particles included (1) roasting in vacuum at 300°C for 1 h, (2) oxidation by 5% NaOCl solution in an oxygen-free environment for 12 h, or (3) oxidation by plasma radiation (<100°C) in air or under a N_2 atmosphere for 1.5 h.

All treatments gave $\delta^{18}O$ and $\delta^{13}C$ values lower than nontreated samples (Table 2). If the samples were not treated, the oxygen and carbon isotopes of the natural siderite were not affected by additions of glucose, spent medium, commercial or biogenic magnetite, or glass fibers (Table 2). These results suggest that glucose, spent medium, or magnetite could exchange isotopic compositions with siderite during the treatments. Other investigators have observed that methods commonly used to remove organic matter could cause significant isotopic offsets (Koch et al., 1997). As a result, all samples reported in this study were analyzed without any oxidative treatment. However, precipitates were washed with distilled water at least three times before being dried in a vacuum dessicator.

Siderite yield was calculated for the natural siderite but not for the biogenic siderite because its absolute concentration in the siderite-magnetite mixture was not determined. The low yield (average 73 $\pm$ 16%) from the nonroasted natural siderite (Table 2) was associated with large reaction vessels used in the early testing. All other nonroasted samples were reacted in sealed Pyrex tubes, most of which gave >90% yield of siderite. On the other hand, three of five roasted samples gave yield <70% of siderite (Table 2). As a result, the Pyrex tubes were used for all experimental samples in this study.

Table 2. Effects of treatments on $\delta^{18}O$ and $\delta^{13}C$ of natural siderite and laboratory-produced biogenic siderite.

Sample	Treatment	Sid. Yield (wt.%)	$\delta^{13}C_{VPDB}$ (‰)	$\delta_{18}O_{VSMOW}$ (‰)
$FeCO_3$[1]	No	73 ± 16 (n = 4)	−4.8 ± 0.2 (n = 4)	10.8 ± 0.1 (n = 4)
$FeCO_3$	Roast@300°C, 1 h	86	−5.22	10.3
$FeCO_3$ + glucose	No	98	−4.7	10.8
$FeCO_3$ + glucose	Roast@300°C, 1 h	59	−6.4	8.8
$FeCO_3$ + spent medium[2]	No	90	−4.8	10.8
$FeCO_3$ + spent medium[2]	Roast@300°C, 1 h	69	−5.1	10.4
$FeCO_3$ + Fisher magnetite	No	91	−4.8	10.8
$FeCO_3$ + Fisher magnetite	Roast@300°C, 1 h	46	−5.4	10.3
$FeCO_3$ + Fisher magnetite + glucose + spent medium[2]	Roast@300°C, 1 h	106	−5.3	10.3
$FeCO_3$ + biogenic magnetite	No	98	−4.8	10.8
$FeCO_3$ + glass fiber	No	92.8	−4.74	10.78
		87.3	−4.63	10.90
Biogenic siderite[3]	No	nd[4]	−3.17	19.94
			−3.20	19.81
Biogenic siderite	Roast@300°C, 1 h	nd	−4.92	16.76
			−4.37	17.34
Biogenic siderite	5% NaOCl, 12 h	nd	−10.77	17.42
		nd	−4.24	18.76
Biogenic siderite	Air-plasma, 1.5 h	nd	−4.1	18.5
Biogenic siderite	N_2-plasma, 1.5 h	nd	−4.4	18.4

The ± values indicate one standard deviation of the mean.
[1] Natural siderite from Brazil; X-ray diffraction pattern showed no other minerals. The origin of the Brazilian siderite is unknown.
[2] Containing metabolic products such as short-chain fatty acids.
[3] Coprecipitated with biogenic magnetite in a TOR-39 culture; X-ray diffraction showed only siderite and magnetite peaks.
[4] Not determined.

Isotopic analysis of siderite was accomplished by reacting a subsample (10–48 mg dry weight) with 100% phosphoric acid in a Pyrex vessel at 60°C. Reaction was terminated after 2 days, at which time CO_2 was no longer produced, and the reaction was considered completed. The evolved CO_2 was used for calculation of siderite abundance in the subsample and for analysis of oxygen and carbon isotope compositions. Because CO_2 has a different oxygen isotope composition than siderite from which the gas was evolved, a fractionation factor ($\alpha_{siderite\text{-}CO2}$) of 1.01006 (Rosenbaum and Sheppard, 1986) was used to back-calculate the isotopic compositions of siderite. Oxygen isotopes of siderite were reported relative to the international standard Vienna-SMOW and carbon isotopes relative to the international standard Vienna-PDB. Oxygen isotope compositions of the medium waters (OR, UM, and W4; Table 1) were analyzed by the CO_2-H_2O equilibration method calibrated against Vienna-SMOW at 25°C (Epstein and Mayeda, 1953). Because our focus was on oxygen isotopes of siderite, only limited carbon-isotope data were collected for total dissolved inorganic carbon, and no data were collected for head-space CO_2. Carbon isotope compositions of the head-space CO_2, however, were calculated by using the fractionation between bicarbonate and CO_2 according to Szaran (1997). All isotopic analyses were performed by using a Finnigan MAT 252 mass spectrometer, which has an internal precision of ± 0.01 to 0.03‰ for both oxygen and carbon isotope analyses.

3. RESULTS

3.1. Solution Chemistry and Mineralogy

3.1.1. Changes in solution chemistry in bacterial cultures and in abiotic controls

In the C1-OR cultures and at 120 mM of bicarbonate concentration, cells increased ≈14-fold within the first 14-h incubation, changing from 1.6×10^7 cells/mL at 0.5 h to 2.4×10^8 cells/mL at 14 h (Fig. 3a). In the C1-W4 cultures, cells increased ≈24-fold, changing from 1.1×10^7 cells/mL at 0.5 h to 2.5×10^8 cells/mL at 14 h (Fig. 3a). Cells began to decrease rapidly in both C1-OR and C1-W4 cultures after 14 h.

The pH decreased during bacterial growth (Fig. 3b). In both cultures, the pH dropped slightly between 0.5 h and 14 h and more markedly between 14 and 168 h. After 168 h, pH decreased much more slowly. The decrease in pH was probably due to the production of organic acids from the breakdown of glucose by the cells of C1 (Fig. 2). The more rapid decrease in pH between 14 and 168 h indicated that the buffering capacity of the bicarbonate perhaps could not keep up with the production of organic acids produced by cells of C1.

The pH also decreased in Control-OR samples (Fig. 3b); however, the overall drop in pH was much less than in the bacterial cultures. The final pH in the Control-OR sample was 7.9, whereas the values were 7.2 to 7.4 in the C1-OR and C1-W4 cultures (Fig. 3b). Nevertheless, the decrease in pH in the Control-OR samples indicated that production of organic acids or CO_2 might be possible from abiotic degradation of glucose under the conditions examined (high temperature and presence of reactive iron). The excursion to a pH 9.3 at 14 h in the Control-OR was unexpected and inconsistent with the chemical reactions described above. Because multiple tubes were used for the experiments, this high pH may reflect high initial pH in this particular sample.

The Eh was low (<−350 mV) in C1-OR and C1-W4 cultures when first measured at 0.5 h (Fig. 3c). These low Eh values were most likely caused by inoculation from low-Eh, pregrown cultures because the control samples not receiving the inoculation had much higher Eh at 0.5 h (−120 mV) (Fig.

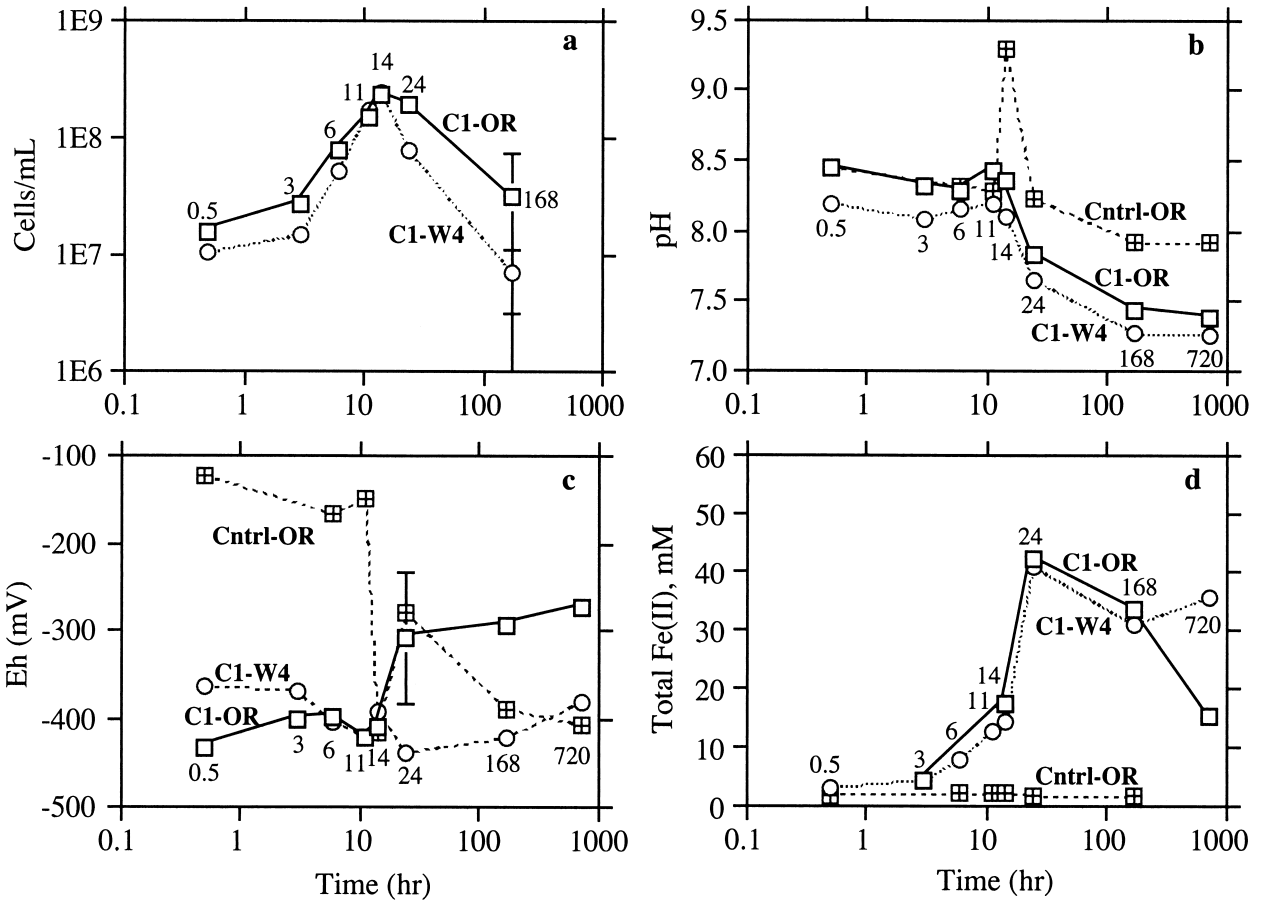

Fig. 3. Changes in cell abundance (a), pH (b), Eh (c), and total Fe(II) (d) as a function of time in bacterial cultures (C1-OR, C1-W4) and in the abiotic control (Cntrl-OR). Both cultures and the abiotic control contained 120 mM of bicarbonate and were incubated at 65°C. Error bars indicate one standard deviation. The timescale is logarithmic so that a better separation can be achieved between data points within the first 24 h. Numbers within the figure were incubation times (same in Figs. 4, 7, and 8).

3c). During incubation, Eh in C1-OR cultures increased slightly from −430 mV at 0.5 h to about −410 mV at 14 h and then increased more markedly to about −310 mV at 24 h (Fig. 3c). After 24 h, Eh increased slowly to about −270 mV at the end of experiment (Fig. 3c). Eh in C1-W4 cultures, on the other hand, decreased gradually from about −360 mV at 0.5 h to about −440 mV at 24 h and then returned to about −380 mV at the end of experiment (Fig. 3c). Eh in Control-OR decreased slightly from −120 mV at 0.5 h to −150 mV at 11 h. It decreased much faster after 11 h and reached a value of −410 mV at the end of experiment (Fig. 3c).

Some of the variations in Eh can be explained by changes in pH because Eh is negatively correlated with pH for many redox reactions. The pronounced increase in Eh between 14 and 24 h in C1-OR was probably due to significant decrease in pH during this period of incubation; the low Eh at 14 h in the Control-OR was probably the result of the high pH (Fig. 3b). Other variations in Eh, however, cannot be explained by changes in pH. For example, in Control-OR, both pH and Eh decreased after 24 h (Figs. 3b and 3c). These results suggest that changes in Eh may be affected by pH and/or other chemical parameters that have yet to be determined.

Total Fe(II) production in C1-OR and C1-W4 cultures was similar and concurrent with cell growth (Fig. 3d). In both cultures, total Fe(II) changed from <5 mM at 0.5 h to ≈40 mM at 24 h and decreased thereafter. Because of mineral precipitation during iron reduction, most of the Fe(II) was fixed in the solid phases (i.e., siderite and magnetite, see next section) and only a small portion (≤3% in most samples) of the iron was in the dissolved phase (Table 3). The final Fe(II) in the C1-OR sample (15.4 mM) was much lower than that in the C1-W4 sample (35.6 ± 2 mM) (Fig. 3d), which was most likely due to the low amount of iron initially added to the tube (C1-OR (S2), Table 4).

Fe(II) was also produced in Control-OR samples. This has been observed previously and was attributed to abiotic reduction of Fe(III) by glucose at higher temperatures (Zhang et al., 1996). The total Fe(II) in the Control-OR samples was <3.0 mM throughout the experiment (Fig. 3d), which included only soluble Fe(II) (0.0–0.25 mM) and siderite Fe(II) (1.7–2.3 mM). Magnetite was also detected in the abiotic samples after 168 h as evidenced by weak attraction of the precipitate to a magnet. With use of techniques of magnetic remnance, the abundance of magnetite in similar control experiments was

Table 3. Production of Fe(II) as a function of time for C1-W4 cultures at 120 mM of bicarbonate concentration (suite 3 experiment, Table 1).

Time (h)	Total Weight (mg)	Siderite (mg)	SI-sid[1]	Fe_3O_4[2] (mg)	Soluble Fe(II)[3] (mM)	Fe(II) of siderite (mM)	Fe(II) of magnetite (mM)	Total Fe(II) (mM)
0.5	82.1	3.8	1.8	na[4]	0.0	3.3	na	3.3
3	91.3	4.3		na	0.1	3.7	na	3.8
3	83.0	5.8	2.5	na	0.1	5.0	na	5.1
6	83.0	8.9		na	0.1	7.7	na	7.8
6	84.0	9.6	3.1	na	0.1	8.3	na	8.4
11	79.8	14.2		na	0.3	12.2	na	12.5
11	79.0	14.9	3.5	na	0.2	12.9	na	13.1
14	79.5	14.7		na	0.3	12.7	na	13.0
14	82.0	17.9	3.4	na	0.2	15.4	na	15.6
24	76.0	18.2		57.8	0.4	15.7	24.9	41.0
24	77.0	16.2	2.8	60.8	0.3	14.0	26.2	40.5
168	65.9	4.5		26.4	0.1	3.9	26.4	30.4
168	68.0	6.0	2.3	26.7	0.1	5.2	26.7	32.0
720	67.8	11.4		24.3	0.1	9.8	24.3	34.2
720	72.0	13.6	2.5	25.2	0.1	11.7	25.2	37.0

All Fe(II) concentrations are normalized to the total volume of solution. SI-sid = saturation index for siderite. SI was not calculated for magnetite.
[1] Estimated from C1-OR samples in suite 2 experiment (Table 1).
[2] Calculated as the difference between total solids and siderite weight. Magnetite began to precipitate at 11-h incubation (see Fig. 5); its contribution to total reduced iron at this time was small because iron oxyhydroxide was still abundant. After 24 h, the total solids were assumed to consist of only siderite and magnetite on the basis of X-ray diffraction patterns (Fig. 5).
[3] Soluble Fe(II) accounted for ≤3% of total Fe(II) at each sampling time.
[4] Not available.

<2% of total solids (Zhang et al., manuscript in preparation). This would give ≈0.6-mM Fe(II) from magnetite in addition to Fe(II) from the solution and siderite. Overall, iron reduction in the abiotic control was significantly less than in the bacterial cultures (Fig. 3d). This finding suggested that iron reduction was substantially enhanced by bacterial growth in the C1-OR and C1-W4 cultures.

Additional time-course experiments were performed at 60 mM of bicarbonate to examine the effect of bacterial growth on solution chemistry and isotope fractionation (suites 4 and 5, Table 1). Two concentrations of inocula were used: 1.7×10^5 cells/mL (0.1%) and 7.6×10^6 cells/mL (10%). Although more biomass was produced with the greater amount of inoculum (Fig. 4a), the resulting changes in pH and total Fe(II) were

Table 4. Summary of Fe(II) species in C1 cultures at the end of experiments (240–720 h).

Sample ID	Temp (°C)	Initial HCO_3^- (mM)	Final pH	Total Solids (mg)	Sid (mg)	Sid (%)	Mag (mg)[1]	Mag (%)	Fe(II) in solution[2] (mM)	Fe(II) in siderite[2] (mM)	Fe(II) in magnetite[2] (mM)	Total Fe(II)[3] (mM)	[Fe(II) + Fe(III)][3] (mM)
C1-OR (S2)	65	120	7.4	32.3	3.2	10.0	29.0	90.0	0.14	2.8	12.5	15.4	40.4
C1-W4 (S3)	65	120	7.2	69.9	12.5	17.9	57.4	82.1	0.09	10.8	24.7	35.6	85.1
C1-OR (S4)	65	60	7.5	37.0	1.8	4.8	35.2	95.2	0.15	1.5	15.2	16.9	47.2
C1-OR (S5)	65	60	7.3	41.5	2.8	6.7	38.7	93.3	0.40	2.4	16.7	19.5	52.9
C1-OR (S6)	65	10	5.9	37.0	0.3	0.8	36.7	99.2	1.24	0.3	15.8	17.3	49.0
C1-OR (S6)	65	30	6.4	52.8	0.8	1.6	52.0	98.4	0.39	0.7	22.4	23.5	68.3
C1-OR (S6)	65	60	7.2	57.1	5.4	9.4	51.7	90.6	0.26	4.6	22.3	27.2	71.8
C1-OR (S6)	65	240	6.9	53.3	2.0	3.8	51.3	96.2	0.44	1.7	22.1	24.2	68.4
C1-OR (S7)	45	120	7.6	34.0	7.3	21.3	26.8	78.7	0.13	6.3	11.5	17.9	41.0
C1-OR (S7)	55	120	7.5	34.6	5.0	14.3	29.7	85.7	0.10	4.3	12.8	17.1	42.7
C1-OR (S7)	55	120	7.5	39.5	4.4	11.2	35.1	88.8	0.09	3.8	15.1	19.0	49.3
C1-OR (S7)	75	120	7.8	54.7	15.5	28.3	39.2	71.7	0.08	13.3	16.9	30.3	64.1
C1-W4 (S8)	45	120	7.7	43.0	23.6	54.8	19.4	45.2	0.07	20.3	8.4	28.8	45.5
C1-W4 (S8)	55	120	7.5	45.0	6.5	14.4	38.5	85.6	0.11	5.6	16.6	22.3	55.5
C1-W4 (S8)	75	120	7.4	55.8	9.6	17.2	46.2	82.8	0.06	8.3	19.9	28.2	68.1

Numbers in parentheses (such as S2) in column 1 are suite numbers of experiments defined in Table 1. All Fe(II) and Fe(III) concentrations are normalized to the total volume of solution.
[1] The abundance of magnetite (Mag) in milligram (mg) was calculated as the difference between total solids and siderite (Sid) assuming magnetite and siderite were the only phases after a 24-h incubation.
[2] Fe(II) in solution was measured by using the ferrozine method. Fe(II) in siderite (mM) was calculated on the basis of the sample weight (mg) and formula weight (116) of siderite and a volume of 10 mL. Fe(II) in magnetite (mM) was calculated on the basis of the sample weight (mg) and formula weight (232) of magnetite and a volume of 10 mL.
[3] Total Fe(II) is the sum of Fe(II) in solution, Fe(II) in siderite, and Fe(II) in magnetite. Total iron is the sum of total Fe(II) plus the Fe(III) in magnetite.

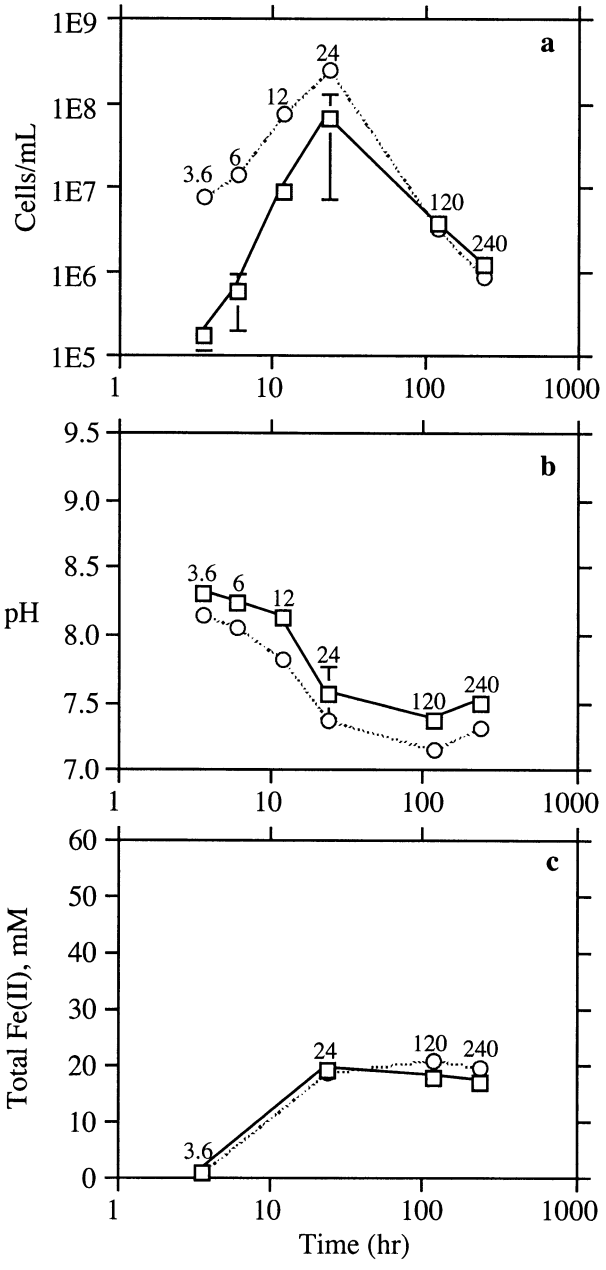

Fig. 4. Changes in cell abundance (a), pH (b), and total Fe(II) (c) as a function of time in C1-OR cultures of two different inoculation concentrations: circles, 7.6×10^6 cells/mL; squares, 1.7×10^5 cells/mL. Cultures had 60 mM of initial bicarbonate and were incubated at 60°C. Error bars indicate one standard deviation.

similar between the two experiments (Figs. 4b and 4c). This finding suggested that increase in bacterial biomass did not significantly affect the solution chemistry under the conditions examined. The final pH values in these experiments were close to those in C1-OR and C1-W4 in Figure 3b. The total Fe(II) values at the end, however, were lower than that in the C1-W4 culture (Fig. 3d). These low values were again due to low total iron initially added to the tubes (C1-OR (S4) and C1-OR (S5), Table 4).

Final pH and Fe(II) from all C1 culture experiments were

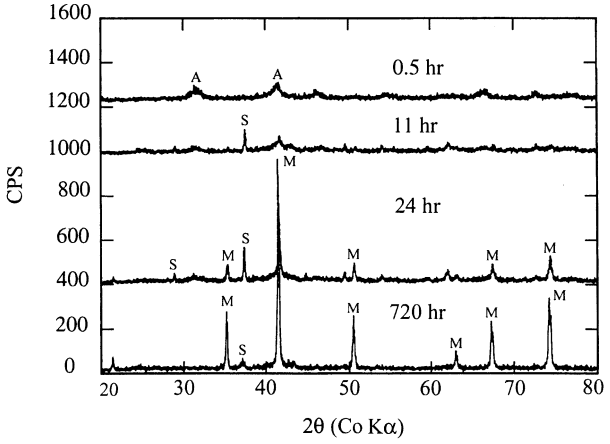

Fig. 5. X-ray diffraction patterns of the iron minerals formed in C1-OR cultures at 65°C and 120 mM of initial bicarbonate. A = akaganeite. S = siderite. M = magnetite.

summarized in Table 4. The results indicated that significantly lower pH (≤6.4) occurred in samples having initial HCO_3^- of ≤ 30 mM, which also had the lowest amount of siderite (Table 4). Overall, the total Fe(II) varied from 15.4 to 35.6 mM in the final samples, which accounted for 34 to 47% of total iron (Fe(II) + Fe(III)). There was one exception of much higher Fe(II) (63%) that occurred in a C1-W4 sample at 45°C (Table 4).

3.1.2. Changes in mineralogy in bacterial cultures and in abiotic controls

Calculations of saturation indices indicated that the solution was supersaturated with respect to siderite from the beginning and throughout the course of the experiments (Table 3). The formation of siderite and magnetite during bacterial iron reduction was confirmed by X-ray diffraction (Fig. 5) and scanning electron microscopy (Fig. 6). The XRD patterns showed a small amount of nonmagnetic akaganeite in the bulk phase of amorphous ferric oxyhydroxide at 0.5 h (Fig. 5). Although CO_2 yields measured from reaction of total solids with phosphoric acid indicated the presence of carbonate in the solids at this time (Table 3), siderite was not detected by the X-ray diffraction before 11 h.

After 11 h, the precipitate became weakly magnetic, and XRD showed the presence of siderite and a small peak of magnetite (Fig. 5). After 24 h, the precipitates became strongly magnetic, and the XRD patterns showed major peaks of magnetite and smaller peaks of siderite (Fig. 5). Note that the akaganeite peaks almost completely disappeared at 24 h, indicating the production of siderite and magnetite and the consumption of the ferric oxyhydroxide. After 720 h, magnetite peaks became predominant, whereas the siderite peaks became even less intense (Fig. 5). Under SEM, siderite crystals (3–5 μm) in the C1-OR samples were rhombohedral in shape and coated with fine-grained magnetite (Fig. 6). Siderite particles were only observed in samples after 11 h, which was consistent with the X-ray diffraction data. The size of siderite crystals did not seem to vary noticeably with incubation time (data not shown). Because the solids consisted of mostly siderite and

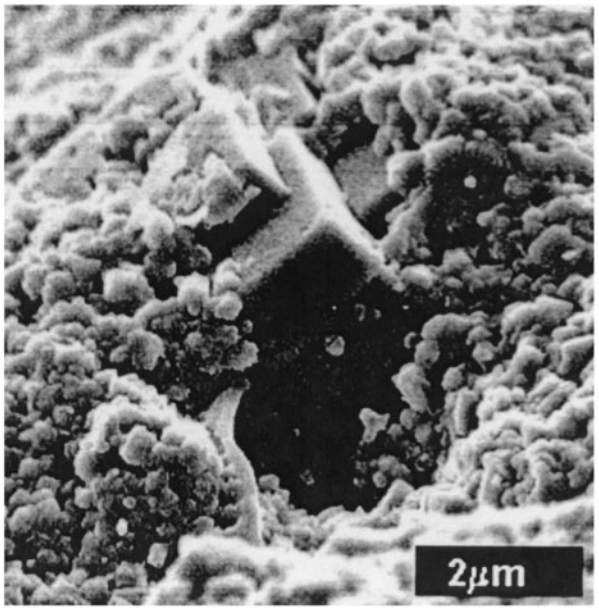

Fig. 6. A large siderite crystal (center) formed in a C1-OR culture at 65°C and 240 mM of bicarbonate after a 720-h incubation. The siderite crystal was covered with finer grains of coprecipitating magnetite.

magnetite after 24 h (Fig. 6), the abundance of magnetite after 24 h can be estimated from the measured siderite and the total solids (Table 3 and Table 4). The results indicated that >70% of the total precipitates were magnetite in most samples (Table 4).

In GS-15 cultures, magnetite and siderite were also the dominant minerals. In the BrY cultures, however, siderite, vivianite, and other unknown iron minerals were produced, but magnetite was not detected. These results indicated that magnetite was not always formed during bacterial iron reduction.

3.2. Oxygen Isotope Compositions of Siderite

A complete list of oxygen isotope compositions of siderite and water is in Table 5. A total of 51 samples were analyzed for $^{18}O/^{16}O$, among which 53% had duplicates (Table 5). These duplicates gave standard deviations ranging from 0.0‰ to 2.6‰ with an average of 0.7 ± 0.7‰ (n = 27). Samples C1-OR 168 h-b and C1-OR 720 h-b (suite 2) and C1-OR 55°C-a (suite 7) were contaminated when they were washed with acetone instead of water. These samples were not included in the calculation of standard deviation and not reported in the following sections. All other samples were clean, judging from mass spectrum after each isotopic run.

3.2.1. Time effect on oxygen isotope compositions of siderite

Effects of incubation time on oxygen isotope compositions of the medium water and siderite were examined in C1-OR, C1-W4, and Control-OR at 120 mM of bicarbonate (Fig. 7). The $\delta^{18}O$ of the medium water remained relatively constant throughout the course of experiments (Figs. 7a–7c). Siderite was always enriched in ^{18}O relative to the medium water, but its $\delta^{18}O$ values decreased with time in both culture samples and

Table 5. Summary of oxygen isotope compositions of siderite and water for the 11 suites of experiments performed in this study (Table 1).

Sample	Time (h)	Temp (°C)	HCO_3^- (mM)	$\delta^{18}O_{H2O}$ (‰)	$\delta^{18}O_{Sid}$ (‰)	$10^3 ln\alpha_{sid\text{-}H_2O}$ (‰)
Suite 1						
Contr-OR	0.5	65	120	−4.9	24.3	29.0
Contr-OR	6	65	120	−4.8	22.9	27.5
Contr-OR	11	65	120	−5.1	22.5	27.4
Contr-OR	14	65	120	−5.3	22.5	27.6
Contr-OR	24	65	120	−6.2	22.4	28.4
Contr-OR	168	65	120	−5.2	19.1	24.1
Contr-OR	720	65	120	−5.2	18.4	23.4
Contr-OR	500	95	30	−5.6	11.5	17.1
Suite 2						
C1-OR	0.5	65	120	na[1]	na	na
C1-OR[2]	3a	65	120	na	na	na
C1-OR	3b	65	120	na	na	na
C1-OR	6a	65	120	na	na	na
C1-OR	6b	65	120	na	na	na
C1-OR[2]	11a	65	120	−5.3	28.6	33.5
C1-OR	11b	65	120	na	na	na
C1-OR[2]	14a	65	120	−4.8	26.8	31.3
C1-OR	14b	65	120	na	na	na
C1-OR[2]	24a	65	120	−4.8	28.3	32.7
C1-OR[2]	24b	65	120	−5.3	28.6	33.5
C1-OR[2]	168a	65	120	−4.6	20.3	24.7
C1-OR[2]	168b	65	120	−5.2	30.9[3]	nd[4]
C1-OR[2]	720a	65	120	−5.3	18.9	24.0
C1-OR[2]	720b	65	120	−5.3	22.5[3]	nd
Suite 3						
C1-W4	0.5a	65	120	−26.6	10.7	37.6
C1-W4	0.5b	65	120	−29.1	na	na
C1-W4	3a	65	120	−28	7.6	36.0
C1-W4	3b	65	120	−28.9	7.4	36.8
C1-W4	6a	65	120	−28.4	6.5	35.4
C1-W4	6b	65	120	−29.2	6.5	36.1
C1-W4	11a	65	120	−26.3	5.6	32.3
C1-W4	11b	65	120	−29.0	5.3	34.8
C1-W4	14a	65	120	−28.0	5.3	33.7
C1-W4	14b	65	120	−28.1	5.2	33.7
C1-W4	24a	65	120	−28.9	4.8	34.1
C1-W4	24b	65	120	−28.6	5.1	34.1
C1-W4	168a	65	120	−27.6	−4.2	23.8
C1-W4	168b	65	120	−28.9	−4.7	24.6
C1-W4	720a	65	120	−28.5	−4.9	24.0
C1-W4	720b	65	120	−28.8	−5.5	23.7
Suite 4						
C1-OR	3.6a	65	60	−7.5	18.0	25.4
C1-OR	3.6b	65	60	−7.6	14.2	21.7
C1-OR	6a	65	60	nd	nd	nd
C1-OR	6b	65	60	nd	nd	nd
C1-OR	12a	65	60	nd	nd	nd
C1-OR	12b	65	60	nd	nd	nd
C1-OR	24a	65	60	−7.3	11.4	18.7
C1-OR	24b	65	60	−7.5	14.0	21.3
C1-OR	120a	65	60	−7.6	15.0	22.4
C1-OR	120b	65	60	−7.4	14.1	21.4
C1-OR	240a	65	60	−7.1	13.3	20.3
C1-OR	240b	65	60	−7.0	14.0	21.0
Suite 5						
C1-OR	3.6a	65	60	−7.2	14.5	21.6
C1-OR	3.6b	65	60	−7.2	14.9	22.0
C1-OR	6a	65	60	nd	nd	nd
C1-OR	6b	65	60	nd	nd	nd
C1-OR	12a	65	60	nd	nd	nd
C1-OR	12b	65	60	nd	nd	nd
C1-OR	24a	65	60	−7.1	12.6	19.6
C1-OR	24b	65	60	−7.1	14.0	21.0

(continued)

Table 5. (Continued)

Sample	Time (h)	Temp (°C)	HCO_3^- (mM)	$\delta^{18}O_{H2O}$ (‰)	$\delta^{18}O_{Sid}$ (‰)	$10^3 ln\alpha_{sid\text{-}H_2O}$ (‰)
Suite 5						
C1-OR	120a	65	60	−7.5	14.6	22.0
C1-OR	120b	65	60	−7.1	14.6	21.0
C1-OR[2]	240a	65	60	−7.0	14.2	21.0
C1-OR[2]	240b	65	60	−7.1	14.6	21.6
Suite 6						
C1-OR[2]	720	65	10a	−5.9	na	na
C1-OR	720	65	10b	−5.2	16.4	21.5
C1-OR[2]	720	65	30a	−5.2	18.2	23.3
C1-OR	720	65	30b	−4.5	na	na
C1-OR	552	65	30c	−6.4	16.0	22.3
C1-OR[2]	720	65	60a	−4.5	20.2	24.6
C1-OR	720	65	60b	−4.8	20.2	24.8
C1-OR	720	65	240a	−5.3	19.3	24.5
C1-OR	720	65	240b	−5.3	19.0	24.1
Suite 7						
C1-OR[2]	720	45a	120	−4.7	22.6	27.0
C1-OR	720	45b	120	−4.7	22.7	27.1
C1-OR[2]	720	55a	120	−4.7	26.0[3]	nd
C1-OR[2]	720	55b	120	−4.8	21.4	25.9
C1-OR[2]	720	75a	120	−5.4	18.2	23.5
C1-OR[2]	720	75b	120	−4.6	18.0	22.5
Suite 8						
C1-W4	720	45a	120	−28.4	−2.1	26.8
C1-W4	720	45b	120	−28.9	−2.4	27.0
C1-W4	720	55a	120	−28.6	−3.6	25.4
C1-W4	720	55b	120	−29.0	−3.7	25.8
C1-W4	720	75a	120	−28.4	−5.9	22.9
C1-W4	720	75b	120	−28.7	−6.4	22.7
Suite 9a						
TOR-39-OR	552	65	30	−4.8	19.1	23.7
Suite 9b						
M3-H2-OR	500	65	30	−4.7	21.0	25.5
Suite 10						
GS-15-UM[2]	500	210	30	−9.5	22.1	31.4
GS-15-UM[2]	500	30	30	−9.4	19.4	28.6
Suite 11						
BrY-OR[2,5]	500	10	60	−5.8	30.8	36.2
BrY-OR[2,5]	500	25	60	−6.7	10.1	16.8
BrY-OR[2]	500	25	60	−5.6	25.6	30.9
BrY-OR	500	10a	60	−6.3	20.8	26.9
BrY-OR	500	10b	60	−6.3	22.3	28.4
BrY-OR	500	37a	60	−6.1	20.7	26.6
BrY-OR	500	37b	60	−6.6	20.7	27.1

Oxygen isotope compositions of water (H_2O) and siderite (sid) were reported relative to the international standard VSMOW.

[1] Not available due to the loss or small sizes of samples.

[2] Samples washed with acetone. All others were washed with distilled water.

[3] Contamination and not used for figure plotting and discussion.

[4] Not determined.

[5] Ferric citrate (25 mM) was used as the electron acceptor instead of amorphous iron.

in the abiotic controls (Figs. 7a–7c). As a result, the fractionation between siderite and water decreased with time, changing from 32.8‰ (3 h) to 24.0‰ (720 h) in C1-OR (Fig. 7a), from 37.6‰ (0.5 h) to 23.8‰ (720 h) in C1-W4 (Fig. 7b), and from 29.0‰ (0.5 h) to 23.4‰ (720 h) in Control-OR (Fig. 7c).

The fractionations in C1-OR and C1-W4 cultures were significantly higher than those in the Control-OR samples during the first 24 h (Fig. 8). This was also the time when bacterial cells grew exponentially (Fig. 3a). After 24 h, the differences in fractionation between culture samples and abiotic controls became smaller. After 168 h, the difference had essentially diminished (Fig. 8).

The pronounced decrease in fractionation with incubation time, however, was not observed in experiments at 60 mM of bicarbonate (Fig. 8). At 7.6×10^6 cells/mL inoculation, the fractionation varied from 21.8‰ at 3.6 h to 21.3‰ at 240 h; at 1.7×10^5 cells/mL inoculation, the fractionation varied between 23.5‰ and 20.6‰ during the same period of incubation (Fig. 8). Overall, the difference in fractionation between the two experiments was statistically insignificant, even though there was more biomass with the greater amount of inoculum (Fig. 4a). This suggests that in these experiments (60 mM of bicarbonate), different biomass or microbial growth did not affect the fractionation between siderite and water. The fractionation values in these experiments, however, were smaller than those with 120 mM of initial bicarbonate (Fig. 8).

3.2.2. Bicarbonate effect on oxygen isotope compositions of siderite

The effect of bicarbonate on isotope fractionation was further evaluated by using C1-OR cultures at 10, 30, 60, and 240 mM of bicarbonate after 720-h incubation (Fig. 9). The results indicated that the oxygen isotope fractionation was small when the initial bicarbonate was low. For example, the $10^3 ln\alpha_{sid\text{-}H2O}$ was 21.5‰ at 10 mM of bicarbonate and was 22.8‰ at 30 mM of bicarbonate. The $10^3 ln\alpha_{sid\text{-}H2O}$ was similar, however, at 60 mM (24.7‰), 120 mM (24.0‰, from time-course experiments), and 240 mM (24.3‰) of bicarbonate (Fig. 9). In C1-W4 and the Control-OR experiments (120 mM of bicarbonate, 720 h), the $10^3 ln\alpha_{sid\text{-}H2O}$ values were slightly smaller than those in the C1-OR experiment at the same bicarbonate concentration (Fig. 9). These experiments plus the time-course experiments at 60 mM of bicarbonate (Fig. 8) indicated that oxygen isotope fractionation tended to decrease when bicarbonate was ≤60 mM.

3.2.3. Effect of incubation temperature on oxygen isotope compositions of siderite

The temperature effect was examined by using samples collected after 240 to 720 h because at these time points the isotope compositions of siderite had approached relatively constant values (Fig. 8). Results showed a general trend of temperature-dependent fractionation at 10 to 95°C (Fig. 10). In particular, The C1-W4 samples at 120 mM of bicarbonate gave good reproducibility (n = 2) at all four temperatures: 26.9 ± 0.1‰ at 45°C, 25.6 ± 0.2‰ at 55°C, 23.8 ± 0.2‰ 65°C, and 22.8 ± 0.2‰ at 75°C (Fig. 11). The fractionation values of C1-OR samples at 120 mM of bicarbonate were consistent with those of the C1-W4 samples. Collectively, these data provided a best fit between the fractionation and temperature at 45 to 75°C, which can be described by the following equation:

$$10^3 \ln\alpha_{sid\text{-}wt} = 2.56 \times 10^6 T^{-2}(K) + 1.69 \quad (r^2 = 0.972) \tag{1}$$

As the number of samples increased, some fractionations deviated below the general trend (Fig. 10). In the C1-OR samples,

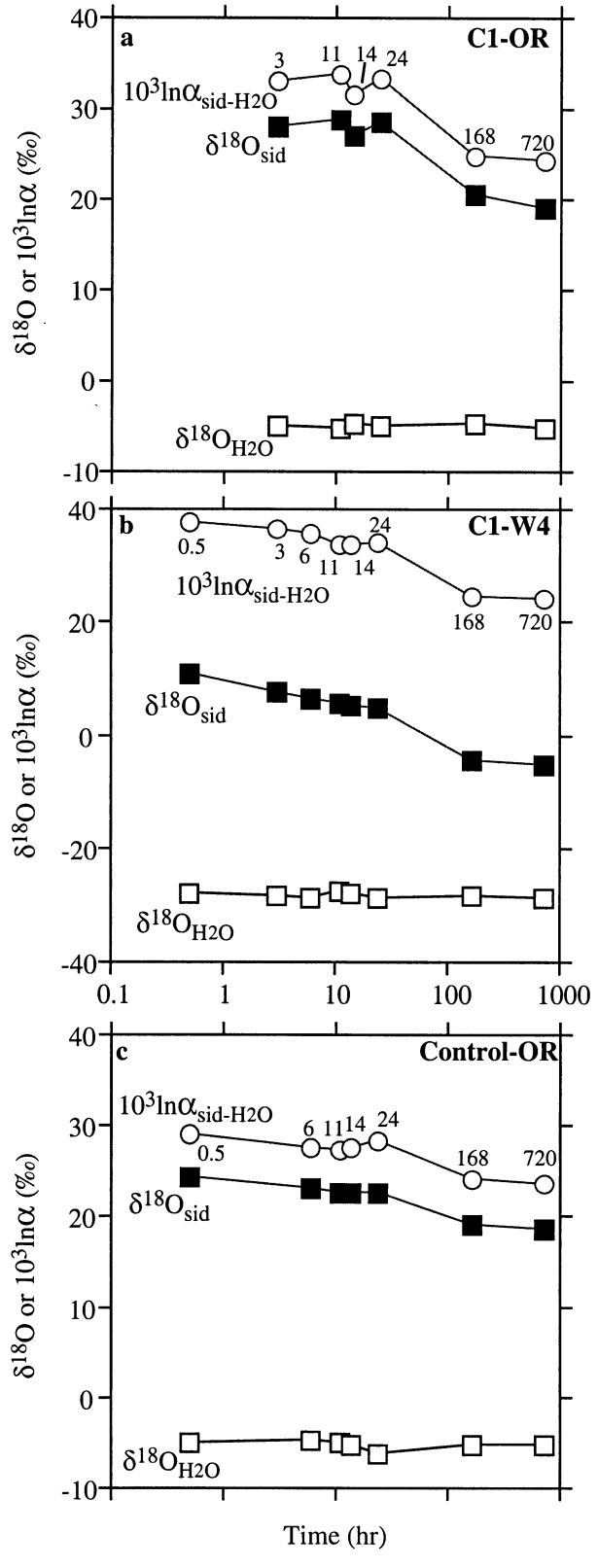

Fig. 7. Oxygen isotopic compositions of siderite (sid) and water (H_2O) and the fractionation between the two as a function of time at 65°C and 120 mM of initial bicarbonate concentration. Data represent average values ± one standard deviation when duplicate samples were available.

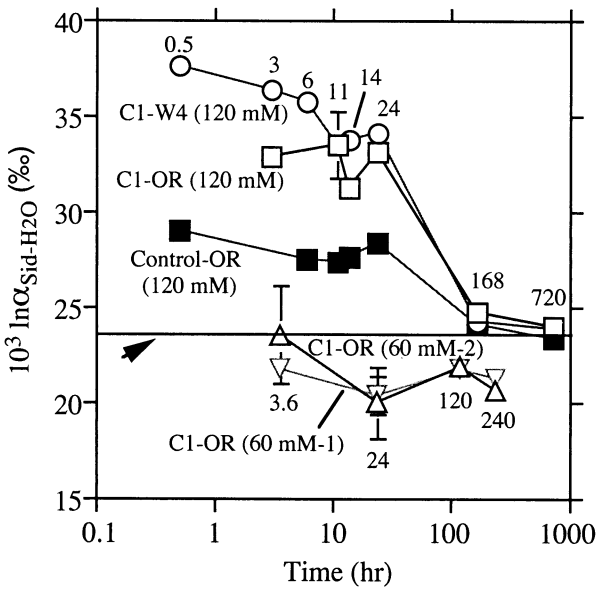

Fig. 8. Summary of oxygen isotope fractionation at 65°C as a function of time in bacterial cultures (C1-OR, C1-W4) and abiotic controls (Control-OR) at two initial bicarbonate concentrations (120 mM and 60 mM). C1-OR (120 mM) and C1-W4 (120 mM) had similar inocula, which were 1.6×10^7 cells/mL and 1.1×10^7 cells/mL, respectively. C1-OR (60 mM-1) had 1.7×10^5 cells/mL inoculum concentration and C1-OR (60 mM-2) had 7.6×10^6 cells/mL inoculum concentration. Also shown is the fractionation (23.9‰, arrow-pointed line) at 65°C for inorganically precipitated siderite based on fractionation factor of Carothers et al. (1988).

the smaller fractionations (<23‰) at 65°C were related to low bicarbonate (10–30 mM after 720 h or 60 mM after 240 h) (Figs. 8 and 9). In the BrY-OR samples, small fractionations may be associated with lower siderite abundance, which in turn

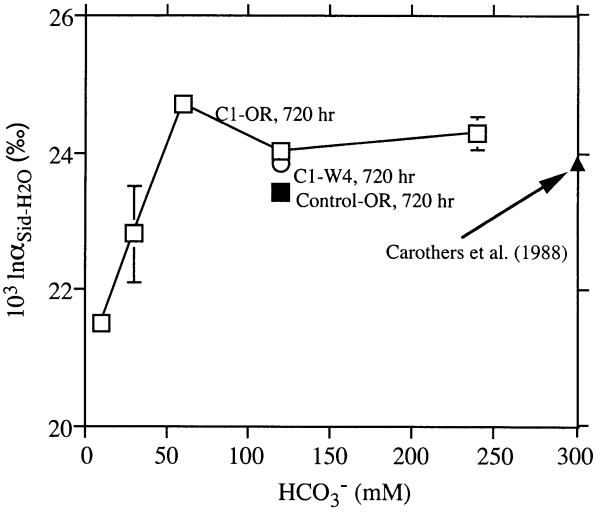

Fig. 9. Oxygen isotope fractionation between siderite and water (65°C) as a function of initial bicarbonate concentrations. Also shown is the fractionation (23.9‰) at 65°C for inorganically precipitated siderite based on fractionation factor of Carothers et al. (1988), who used 300 mM of bicarbonate in their experiments.

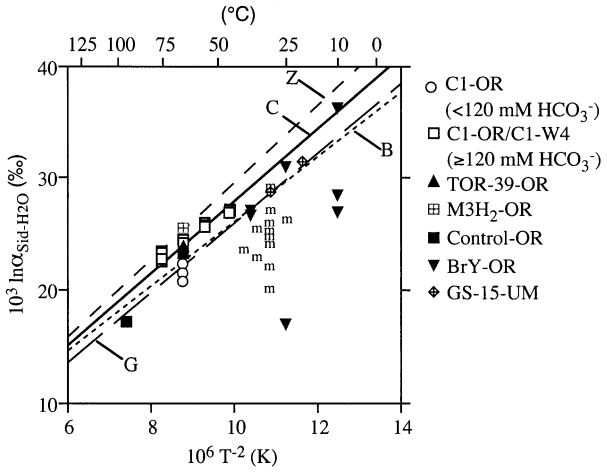

Fig. 10. Oxygen isotope fractionation as a function of temperature for all samples collected at the end of experiments (240–720 h), which were compared with biogenic siderite from Mortimer and Coleman (1997), inorganically precipitated siderite from Carothers et al. (1988), and theoretical calculations from Becker and Clayton (1976), Golyshev et al. (1981) and Zheng (1999). See Fig. 1 for more information.

was related to low bicarbonate. At 25°C, for example, the sample with a smaller fractionation (16.8‰) had 2.7% (0.5 mg) siderite, whereas the sample with a larger fractionation (30.9‰) had 43% (14.3 mg) siderite; at 10°C, the two samples with fractionations below 29‰ had siderite abundance <8%, whereas the sample with a fractionation of 36.2‰ had a siderite abundance of 27%. These smaller fractionations suggest an isotope discrimination against the heavy ^{18}O when forming siderite under low-bicarbonate conditions.

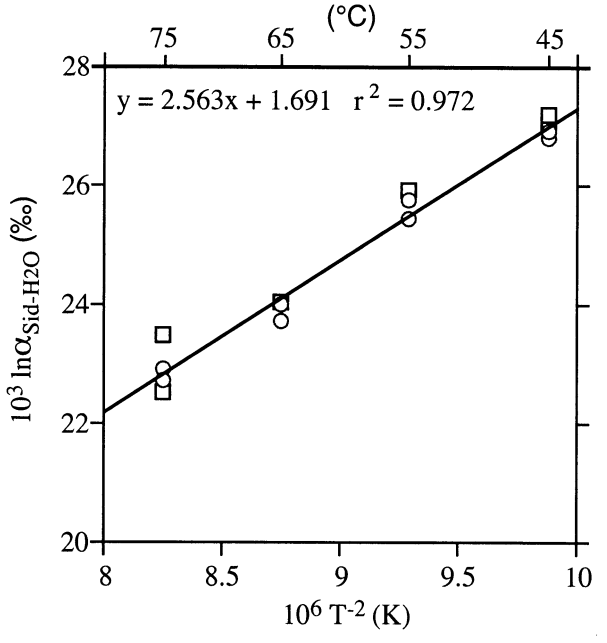

Fig. 11. Oxygen isotope fractionation as a function of temperature at 120 mM of initial bicarbonate and after a 720-h incubation. Open squares, C1-OR cultures; open circles, C1-W4 cultures. The regression line was drawn by using data from both types of cultures.

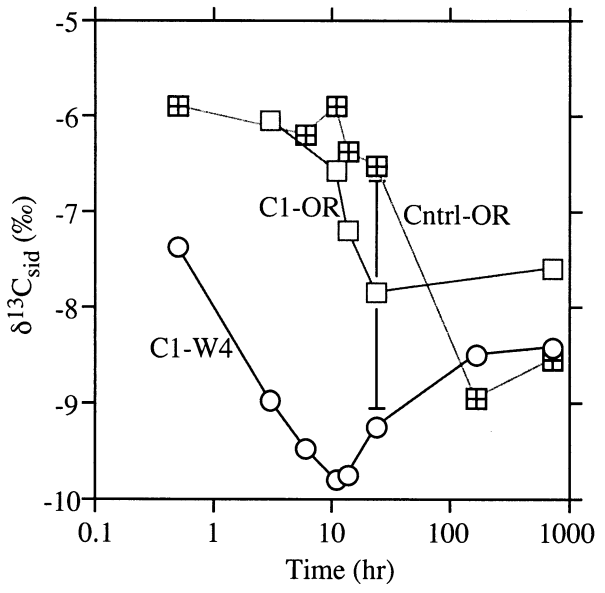

Fig. 12. Carbon isotopic compositions of siderite (sid) as a function of time at 65°C and 120 mM of initial bicarbonate concentration. Data represent average values ± one standard deviation. For C1-W4, the error bars were smaller than the symbols and were not shown.

3.3. Carbon Isotope Compositions of Siderite

The $\delta^{13}C$ of siderite in C1 cultures and in the abiotic controls at 120 mM of bicarbonate also decreased with incubation time (Fig. 12). In C1-OR samples, $\delta^{13}C$ of siderite decreased from −6.0‰ at 3 h to −7.6‰ at 720 h. In Control-OR samples, $\delta^{13}C$ decreased from −6.0‰ at 0.5 h to −8.9‰ at 720 h. In C1-W4 samples, $\delta^{13}C$ decreased from −7.4‰ at 0.5 h to −8.5‰ at 720 h; however, the lowest values (around −9.8‰) occurred between 11 and 14 h (Fig. 12). Similar to oxygen isotope composition, the $\delta^{13}C$ of siderite tended to become constant in each experiment (Fig. 12). Using limited isotopic data of total dissolved inorganic carbon for C1-OR samples, we could calculate the fractionation between siderite and CO_2 at different temperatures collected after 720 h (Table 6). These fractionations are compatible with the trend of carbon isotope fractionation determined for abiotically precipitated siderite by Carothers et al. (1988), but are 5 to 10‰ smaller than theoretical calculations by Golyshev et al. (1981) (Fig. 13). The $\delta^{13}C$ of siderite in GS-15 and BrY cultures varied between −27‰ to −40‰. However, fractionation between siderite and CO_2 was not determined for these samples because $\delta^{13}C$ of the bicarbonate was not known.

4. DISCUSSION

4.1. Oxygen Isotope Fractionation Between Siderite and Water

This study represents one of the few experimental studies of oxygen isotope fractionation between siderite and water at relatively low temperatures (<200°C). Carothers et al. (1988) performed inorganic precipitation experiments by slow titration of a 300 mM of bicarbonate solution with 1500 mM of ferrous chloride in a hydrothermal vessel. Samples were collected at

Table 6. Carbon isotope fractionation between biogenic siderite and gaseous CO_2 in C1-OR samples with 120 mM of initial bicarbonate.

Temp (°C)	$10^3\ln\alpha_{HCO3\text{-}CO2}$[1] (‰)	$\delta^{13}C_{HCO3}$[2] (‰)	$\delta^{13}C_{CO2}$[3] (‰)	$\delta^{13}C_{siderite}$[2] (‰)	$10^3\ln\alpha_{siderite\text{-}CO2}$[4] (‰)
45	6.117	−8.58	−14.61	−7.18	7.47
				−7.26	
55	5.163	−8.66	−13.75	−5.46	7.86
				−6.47	
65	4.209	−8.06	−12.21	−7.51 ± 0.36 (n = 5)	4.75
75	3.255	−8.96	−12.18	−7.27	5.18
				−6.83	

[1] Equilibrium fractionation as a function of temperature calculated using the following equation: $10^3\ln\alpha_{HCO3\text{-}CO2} = -0.0954 \times T\ (°C) + 10.41$ (Szaran, 1997).
[2] Measured values. $\delta^{13}C_{HCO_3}$ was approximated as the isotopic compositions of total dissolved inorganic carbon for a pH range of 7.4 to 7.8.
[3] Calculated by using columns 2 and 3.
[4] Calculated by using column 4 and the average value in column 5.

the end of experiments after 5 to 6 days and analyzed for oxygen isotopic compositions of the siderite. Their results showed temperature-dependent fractionation between the precipitating siderite and water at 33 to 197°C, and varied agreement with theoretical calculations (Fig. 1). Mortimer and Coleman (1997) analyzed biogenic siderite precipitated at 18–40°C in GS-15 cultures incubated for 6 to 48 days. Their fractionation values were smaller than those determined from either inorganically precipitated siderite or the theoretical calculations (Fig. 1) and were thought to be indicative of a microbial origin (Mortimer and Coleman, 1997).

The fractionation data from C1 cultures compared favorably with the empirical curve of Carothers et al. (1988) in the temperature range of 45 to 75°C for samples at ≥120 mM of bicarbonate (Fig. 10). Below 45°C, only two of the seven samples from the BrY-OR cultures still followed the empirical curve. However, the two BrY-OR samples at 37°C and two GS-15-UM samples at 20°C and 30°C fell on the theoretical curves of Becker and Clayton (1976) or Golyshev et al. (1981). The other three samples of BrY-OR at 25°C and 10°C had significantly smaller fractionations than the empirical curve of Carothers et al. (1988) and those derived from theoretical calculations (Fig. 10). The smaller fractionations exhibited by the BrY samples had similar deviations from the theoretical values as those of GS-15 reported by Mortimer and Coleman (1997) (Fig. 10). In addition to a possible biologic origin, these low fractionations may also be caused by changes in chemical conditions of bacterial growth. For example, GS-15 in our study gave fractionations close to abiotic fractionation of Carothers et al. (1988), whereas the same bacterial strain produced lower fractionations in most samples of Mortimer and Coleman (1997), who might have used a different chemical milieu.

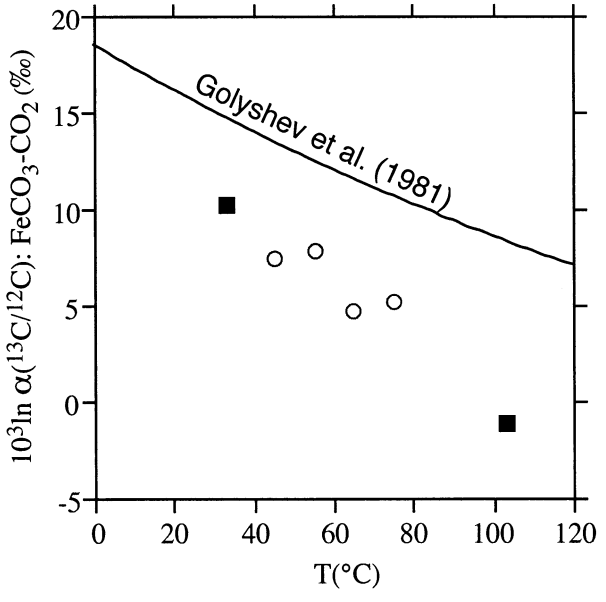

Fig. 13. Carbon isotope fractionation between siderite and CO_2. Circles, this study; squares, Carothers et al. (1988). Also shown is a theoretical curve from Golyshev et al. (1981).

One important finding of this study was the variation in fractionation at different bicarbonate concentrations. During the early precipitation of the solids in the 120 mM of bicarbonate experiments, the fractionation between siderite and water was very high (more positive) but gradually decreased to near constant values (Fig. 8). Even in the control experiment without bacteria, a similar pattern, although less pronounced, was observed (Fig. 8). The patterns were likely due to kinetic processes during early precipitation of siderite or possibly the formation of a Fe(II)Fe(III) hydroxy-carbonate. At 120 mM of bicarbonate, substantial fractions (3–14%) of total dissolved CO_2 including HCO_3^- and $CO_3^=$ precipitated quickly as solid iron carbonates within the first 24 h. This means that all $CO_3^=$ (0.5–1.2% of total dissolved CO_2) initially in the solution was rapidly removed, and the carbonate system had to continuously produce the $CO_3^=$ ion to maintain chemical equilibrium. It is well documented in the literature (Mills and Urey, 1940; Usdowski et al., 1991) that oxygen isotope exchange between dissolved CO_2 and water is orders of magnitudes slower than chemical reactions, depending on temperature and pH. Thus, it is very likely that during the rapid precipitation of iron carbonates at the beginning, the precipitating minerals were not at isotope equilibrium with the water, even though chemical equilibrium might have been maintained throughout.

Kinetic isotope effects have also been observed for other carbonate minerals. Li et al. (1997) reported that when calcite was precipitated instantaneously from an alkaline lake water,

oxygen isotope fractionation factors between calcite and water are ≈10‰ greater than those of expected equilibrium fractionation (Fig. 4 of Li et al., 1997). Kim and O'Neil (1997) observed that isotopic fractionation among nonequilibrium carbonates varied significantly with initial bicarbonate and the higher the metal ion and bicarbonate, the larger the fractionation (up to 3‰ at a given temperature). The magnitude of enrichment reported by Li et al. (1997) was very similar to early fractionation in our experiments at 120 mM of bicarbonate and 65°C (Fig. 8). Li et al. (1997) attributed this enrichment to insufficient isotopic exchange between carbonate crystals and solution due to fast crystal growth. Similarly, the ^{18}O enrichment in early precipitated iron carbonates in this study may be due to the rapid formation of the minerals. In the 60 mM of bicarbonate experiments at 65°C, there was no clear trend of isotope fractionation with incubation time (Fig. 8). Siderite formed in these experiments might simply reflect a slow precipitation.

Although it is not possible to prove that siderite precipitated from solution has reached isotopic equilibrium with water, general trends of $\delta^{18}O$ values of siderite with incubation time suggested that siderite at 120 mM of bicarbonate may have approached isotopic equilibrium with water after 168 h (Fig. 8). In particular, the C1-culture experiments with W4 water showed a good linear relation with incubation temperature (Fig. 11), and its temperature dependence is almost the same as observed by Carothers et al. (1988) for equilibrium fractionation between inorganic siderite and water in the same temperature range (Fig. 11). These results corroborate the findings of Zhang et al. (1997) and Mandernack et al. (1999), who showed temperature-dependent fractionations between biogenic magnetite and water.

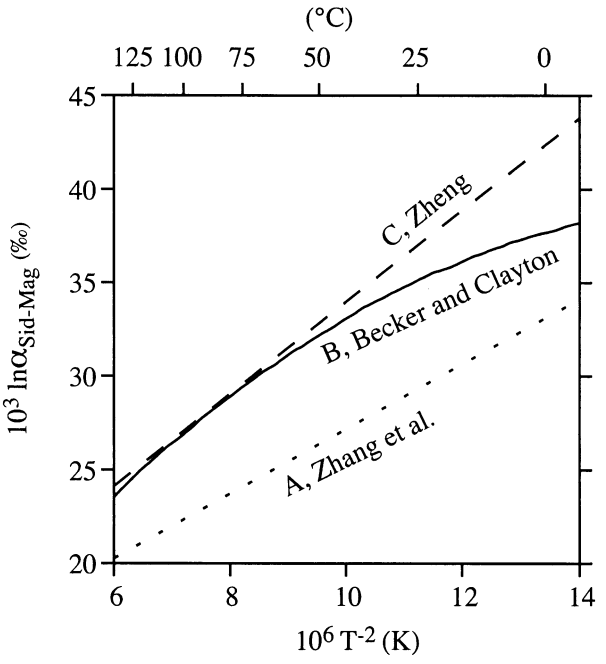

Fig. 14. Oxygen isotope fractionation between siderite and magnetite derived from experimental measurements (curve A) and theoretical calculations (curves B and C). Curve A is obtained by combining the siderite-water fractionation of this study with the magnetite-water fractionation of Zhang et al. (1997). Curve B is obtained by combining the siderite-water and magnetite-water fractionations reported in Becker and Clayton (1976). Curve C is obtained by combining the siderite-water and magnetite-water fractionations reported in Zheng (1991; 1999).

4.2. Geological Implications

Microbial iron reduction is a major respiratory process in low-temperature sedimentary environments (Lovley, 1991; Nealson and Saffarini, 1994). Siderite and magnetite can coprecipitate during iron reduction under the same condition (Zhang et al., 1997). This provides an opportunity to establish a geothermometer based on oxygen isotope fractionation between the two coexisting minerals. Coprecipitation of siderite and magnetite might have occurred widely in the Precambrian-banded iron formations (Eugster and Chou, 1973; Perry et al., 1973; Becker and Clayton, 1976; Klein and Bricker, 1977) and has been observed in a Devonian ironstone (Hangari et al., 1980). Although theoretical calculations of temperature-dependent fractionation exist for siderite-water and magnetite-water pairs (O'Neil and Clayton, 1964; Becker and Clayton, 1976; Golyshev et al., 1981; Zheng, 1991; Rowe et al., 1994), no experimental data are available for oxygen isotope fractionation between coexisting siderite and magnetite. Here we provide a preliminary equation of temperature-dependent fractionation between biogenic siderite and magnetite formed under laboratory conditions:

$$10^3 \ln\alpha_{\text{sid-mag}} = 1.76 \times 10^6 T^{-2}(K) + 9.43 \qquad (2)$$

Eqn. 2 is derived by combining the siderite-water pair (Eqn. 1) of this study with the magnetite-water pair ($10^3 \ln\alpha_{\text{mag-wt}} = 0.80 \times 10^6\ T^{-2}\ (K) - 7.74$) reported by Zhang et al. (1997). Both magnetite and siderite were formed at a temperature range of 45 to 75°C but from different culture samples. Analysis of coexisting siderite and magnetite from the same culture is needed to validate this empirical equation, which will be done in future studies. We also compared Eqn. 3 to siderite-magnetite fractionation calculated from existing data in the literature (Fig. 14). The results show that fractionations between siderite and magnetite of our experimental measurements are 3.8 to 8.7‰ smaller than siderite-magnetite fractionations from theoretical calculations (Fig. 14).

A geothermometer based on coexisting siderite and magnetite may be particularly useful because their isotope compositions can be much better preserved in the geologic record than fluids from which these minerals were originally precipitated. Hangari et al. (1980) analyzed the oxygen isotope compositions of diagenetic siderite and magnetite coprecipitated in the Upper Devonian ironstones in the Wadi Shatti District, Libya. Using Eqn. 2, we calculated the formation temperatures of these minerals to be in the range of 10 to 76°C. Magnetite $\delta^{18}O$ values were corrected for siderite contamination by a factor of 0.05 based on information provided by Hangari et al. (1980). These temperatures are more realistic than original estimation (45 to 120°C), given the fact that the ironstone was deposited in a fresh or brackish deltaic environment and had not experienced high-temperature metamorphism (Hangari et al., 1980). Another application of the siderite-magnetite isotope pair may be to validate the formation temperatures of iron carbonates

and magnetite in a Martian meteorite, which were proposed as possible biomarkers of past biogenic activities on Mars (McKay et al., 1996).

5. CONCLUSIONS

Oxygen and carbon isotope compositions were determined for biogenic siderite formed in both mesophilic (15 to 35°C) and thermophilic (45 to 75°C) iron-reducing cultures. Oxygen isotope compositions of siderite formed abiotically at 65 and 95°C were also determined. The abiotic siderite had similar oxygen isotope compositions as those of biogenic siderite formed at the same temperature, suggesting that microbial fractionations cannot be distinguished from abiotic fractionations under the conditions examined here.

Temperature appears to be a dominant factor controlling the oxygen isotope fractionation between water and the final siderite precipitate. Fractionations for the biogenic siderite formed at ≥120 mM of bicarbonate and after 500 to 720 h may have reached equilibrium, because they are comparable with equilibrium fractionations of inorganically precipitated siderite (Carothers et al., 1988) and theoretical calculations (Becker and Clayton, 1976; Golyshev et al., 1981; Zheng, 1999). Samples in thermophilic cultures (45 to 75°C) gave the best linear correlation between fractionation and temperature, which can be described as $10^3 \ln\alpha_{\text{sid-wt}} = 2.56 \times 10^6\, T^{-2}\,(K) + 1.69$. These results corroborate the findings of Zhang et al. (1997) and Mandernack et al. (1999), who showed temperature-dependent fractionations between biogenic magnetite and water. Carbon isotope fractionations between biogenic siderite and CO_2, based on limited data, also varied with temperature and were consistent with the inorganically precipitated siderite of Carothers et al. (1988). Other variables, such as isotopic compositions of water, types of bacterial species, or bacterial growth rates, had little effect on the fractionation. Results of this study show that oxygen and carbon isotope fractionations may help constrain formation temperatures of biogenic minerals in low-temperature sedimentary basins where biologic activities always occur.

Associate editor: J. B. Fein

Acknowledgments—We thank Yul Roh for XRD analysis and Dorothy Coffey for SEM analysis. Yiliang Li helped with drawing some of the figures. Drs. Alan Fryar, Max Coleman, Eugene Perry, Yiliang Li, and an anonymous reviewer provided valuable comments on an early version of the manuscript. We thank Dr. Jeremy Fein (the Associate Editor) for handling this manuscript. This research was sponsored by the Division of Chemical Sciences, Geosciences, and Biosciences of the Office of Basic Energy Science and the Office of Fossil Energy, in part through the National Energy Technology Laboratory, of the U.S. Department of Energy managed by UT-Battelle, LLC. CLZ was supported by a Summer Faculty Research Program in 1999 through Oak Ridge Associated Universities.

REFERENCES

Allison J. D., Brown D. S., and Novo-Gradac K. J. (1991) *MINTEQA2/PRODEFA2, a geochemical assessment model for environmental systems: Version 3.0 User's Manual.* EPA/600/3-9/021.

Bahrig B. (1989) Stable isotope composition of siderite as an indicator of the paleoenvironmental history of oil shale lakes. *Palaeogeogr. Palaeoclimat. Palaeoecol.* **70,** 139–151.

Becker R. H. and Clayton R. N. (1976) Oxygen isotope study of a Precambrian banded iron-formation, Hamersley Range, Western Australia. *Geochim. Cosmochim. Acta* **40,** 1153–1165.

Caccavo F., Jr, Blakemore R. P., and Lovley D. R. (1992) A hydrogen-oxidizing, Fe(III)-reducing microorganism from the Great Bay Estuary, New Hampshire. *Appl. Environ. Microbiol.* **58,** 3211–3216.

Carothers W. W., Adami L. H., and Rosenbauer R. J. (1988) Experimental oxygen isotope fractionation between siderite-water and phosphoric acid liberated CO_2-siderite. *Geochim. Cosmochim. Acta* **52,** 2445–2450.

Coleman M. L. and Raiswell R. (1993) Microbial mineralization of organic matter: Mechanisms of self-organization and inferred rates of precipitation of diagenetic minerals. *Phil. Trans. R. Soc. Lond.* **A344,** 69–87.

Curtis C. D., Coleman M. L., and Love L. G. (1986) Pore water evolution during sediment burial from isotopic and mineral chemistry of calcite, dolomite and siderite concretions. *Geochim. Cosmochim. Acta* **50,** 2321–2334.

Duan W. M., Hedrick D. B., Pye K., Coleman M. L., and White D. C. (1996) A preliminary study of the geochemical and microbiological characteristics of modern sedimentary concretions. *Limnol. Oceanogr.* **41,** 1404–1414.

Ellwood B. B., Chrzanowski T. H., Hrouda F., Long G. J., and Buhl M. L. (1988) Siderite formation in anoxic deep-sea sediments: A synergetic bacterially controlled process with important implications in paleomagnetism. *Geology* **16,** 980–982.

Epstein S. and Mayeda T. K. (1953) Variations of ^{18}O content of waters from natural sources. *Geochim. Cosmochim. Acta* **4,** 213–224.

Eugster H. P. and Chou I. M. (1973) The depositional environments of Precambrian banded iron-formations. *Econ. Geol.* **68,** 1144–1168.

Fisher Q. J., Raiswell R., and Marshall J. D. (1998) Siderite concretions from nonmarine shales (Westphalian A) of the Pennines England: Controls on their growth and composition. *J. Sediment. Res.* **68,** 1034–1045.

Fredrickson J. K., Zachara J. M., Kennedy D. W., Dong H., Onstott T. C., Hinman N. W., and Li S.-M. (1998) Biogenic iron mineralization accompanying the dissimilatory reduction of hydrous ferric oxide by a groundwater bacterium. *Geochim. Cosmochim. Acta* **62,** 3239–3257.

Golyshev S. I., Padalko N. L., and Pechenkin S. A. (1981) Fractionation of stable oxygen and carbon isotopes in carbonate systems. *Geochem. Intl.* **18,** 85–99.

Hangari K. M., Ahmad S. N., and Perry E. C., Jr. (1980) Carbon and oxygen isotope ratios in diagenetic siderite and magnetite from Upper Devonian ironstone, Wadi Shatti District, Libya. *Econ. Geol.* **75,** 538–545.

Kim S.-T. and O'Neil J. R. (1997) Equilibrium and nonequilibrium oxygen isotope effects in synthetic carbonates. *Geochim. Cosmochim. Acta* **61,** 3461–3475.

Klein C. and Bricker O. P. (1977) Some aspects of the sedimentary and diagenetic environment of Proterozoic banded iron-formation. *Econ. Geol.* **72,** 1457–1470.

Koch P. L., Tuross N., and Fogel M. L. (1997) The effects of sample treatment and diagenesis on the isotopic integrity of carbonate in biogenic hydroxylapatite. *J. Archaeol. Sci.* **24,** 417–429.

Li H.-C., Stott L. D., and Hammond D. E. (1997) Temperature and salinity effects on ^{18}O fractionation for rapidly precipitated carbonates: Laboratory experiments with alkaline lake water. *Epidoses* **20,** 193–198.

Liu S. V., Zhou J., Zhang C., Cole D. R., Gajdarziska-Josifovska M., and Phelps T. J. (1997) Thermophilic Fe(III)-reducing bacteria from the deep subsurface: The evolutionary implications. *Science* **277,** 1106–1109.

Lovley D. R. (1991) Dissimilatory Fe(III) and Mn(IV) reduction. *Microbiol. Rev.* **55,** 259–287.

Lovley D. R. and Lonergan D. J. (1990) Anaerobic oxidation of toluene, phenol, and p-cresol by the dissimilatory iron-reducing organism, GS-15. *Appl. Environ. Microbiol.* **56,** 1858–1864.

Lovley D. R. and Phillips E. J. P. (1988) Novel mode of microbial energy metabolism: organic carbon oxidation coupled to dissimilatory reduction of iron or manganese. *Appl. Environ. Microbiol.* **54,** 1472–1480.

Lovley D. R., Greening R. C., and Ferry J. G. (1984) Rapidly growing

rumen methanogenic organism that synthesizes coenzyme M and has a high affinity for formate. *Appl. Environ. Microbiol.* **48,** 81–87.

Mandernack K. W., Bazylinski D. A., Shanks III W. C., and Bullen T. D. (1999) Oxygen and iron isotope studies of magnetite produced by magnetotactic bacteria. *Science* **285,** 1892–1896.

McKay D. S., Gibson E. K. Jr., Thomas-Keprta K. L., Vali H., Romanek C. S., Clemett S. J., Chillier X. D. F., Maechling C. R., and Zare R. N. (1996) Search for past life on Mars: Possible relic biogenic activity in Martian meteorite ALH84001. *Science* **273,** 924–930.

Mills G. A. and Urey H. C. (1940) The kinetics of isotopic exchange between carbon dioxide, bicarbonate ion, carbonate ion and water. *J. Am. Chem. Soc.* **62,** 1019–1026.

Moore S. E., Ferrell J. R. E., and Aharon P. (1992) Diagenetic siderite and other ferroan carbonates in a modern subsiding marsh sequence. *J. Sediment. Petrol.* **62,** 357–366.

Mortimer R. J. G. and Coleman M. L. (1997) Microbial influence on the oxygen isotopic composition of diagenetic siderite. *Geochim. Cosmochim. Acta* **61,** 1705–1711.

Mozley P. S. and Carothers W. W. (1992) Elemental and isotopic composition of siderite in the Kuparuk Formation, Alaska: Effect of microbial activity and water/sediment interaction on early pore-water chemistry. *J. Sediment. Petrol.* **62,** 681–692.

Mozley P. S. and Wersin P. (1992) Isotopic composition of siderite as an indicator of depositional environment. *Geology* **20,** 817–820.

Nealson K. H. and Saffarini D. (1994) Iron and manganese in anaerobic respiration: Environmental significance, physiology, and regulation. *Ann. Rev. Microbiol.* **48,** 311–343.

O'Neil J. R. and Clayton R. N. (1964) Oxygen isotope geothermometry. In *Isotopic and Cosmic Chemistry* (eds. H. Craig et al.), pp. 157–168. North Holland.

Perry E. C., Jr., Tan F. C., and Morey G. B. (1973) Geology and stable isotope geochemistry of the Biwabik Iron Formation, northern Minnesota. *Econ. Geol.* **68,** 1110–1125.

Phelps T. J., Raione E. G., White D. C., and Fliermans C. B. (1989) Microbial activity in deep subsurface environments. *Geomicrobiol. J.* **7,** 79–91.

Pye K., Dickson J. A. D., Schiavon N., Coleman M. L., and Cox M. (1990) Formation of siderite-Mg-calcite-iron sulphide concretions in intertidal marsh and sandflat sediments, north Norfolk, England. *Sedimentology* **37,** 325–343.

Rosenbaum J. and Sheppard S. M. F. (1986) An isotopic study of siderites, dolomites and ankerites at high temperatures. *Geochim. Cosmochim. Acta* **50,** 1147–1150.

Rowe M. W., Clayton R. N., and Mayeda T. K. (1994) Oxygen isotopes in separated components of CI and CM meteorites. *Geochim. Cosmochim. Acta* **58,** 5341–5347.

Szaran J. (1997) Achievement of carbon isotope equilibrium in the system HCO_3^- (solution)-CO_2 (gas). *Chem. Geol.* **142,** 79–86.

Usdowski E., Michaelis J., Böttcher M.E., and Hoefs J. (1991) Factors for the oxygen isotope equilibrium fractionation between aqueous and gaseous CO_2, carbonic acid, bicarbonate, and water(19°C). *Zeit. Phys. Chem.* **170,** 237–249.

Vargas M., Kashefi K., Blunt-Harris E. L., and Lovley D. R. (1998) Microbiological evidence for Fe(III) reduction on early Earth. *Nature* **395,** 65–67.

Zhang C., Liu S., Logan J., Mazumder R., and Phelps T. J. (1996) Enhancement of Fe(III), Co(III), and Cr(VI) reduction at elevated temperatures and by a thermophilic bacterium. *Appl. Biochem. Biotechnol.* **57/58,** 923–932.

Zhang C., Liu S., Phelps T. J., Cole D. R., Horita J., Fortier S. M., Elless M., and Valley J. W. (1997) Physiochemical, mineralogical, and isotopic characterizations of magnetic iron oxides formed by thermophilic Fe(III)-reducing bacteria. *Geochim. Cosmochim. Acta* **61,** 4621–4632.

Zhang C., Stapleton R. D., Zhou J., Palumbo A. V., and Phelps T. J. (1999) Iron reduction by psychrophilic enrichment cultures. *FEMS Microbiol. Ecol. Lett.* **30,** 367–371.

Zhang C., Vali H., Romanek C. S., Phelps T. J., and Liu S. V. (1998) Formation of single-domain magnetite by a thermophilic bacterium. *Am. Mineral.* **83,** 1409–1418.

Zheng Y. F. (1991) Calculation of oxygen isotope fractionation in metal oxides. *Geochim. Cosmochim. Acta* **55,** 2299–2307.

Zheng Y.-F. (1999) Oxygen isotope fractionation in carbonate and sulfate minerals. *Geochem. J.* **33,** 109–126.